A&A 415, 477–481 (2004)
DOI: 10.1051/0004-6361:20034313

Astronomy & Astrophysics

Parsec-scale rotation-measure distribution in the quasar 3C 147 at 8 GHz

H. Y. Zhang[1], D. C. Gabuzda[2], R. D. Nan[1], and C. J. Jin[1]

[1] National Astronomical Observatories, Chinese Academy of Science, A20 Datun Road, Chaoyang District, Beijing 100012, PR China
[2] Department of Physics, University College Cork, Cork, Ireland

Received 12 September 2003 / Accepted 28 October 2003

Abstract. VLBA polarization observations of the high-rotation-measure source 3C 147 were made at four frequencies in the available 8 GHz band. The distribution of total flux and rotation measure across the source has been imaged. The rotation measure of the inner jet of the source (~ -1800 rad m^{-2}) is consistent with previous results. After removing the rotation of the plane of polarization due to a foreground screen, the derived intrinsic magnetic field structure of the source on parsec scales is roughly transverse to the predominant jet direction, indicating the presence of relativistic shocks or a dominant toroidal jet B-field component.

Key words. polarization – galaxies: jets – galaxies: magnetic fields – galaxies: quasars: individual: 3C 147

1. Introduction

As a typical compact steep-spectrum (CSS) radio source, the quasar 3C 147 ($z = 0.545$) has undergone a large amount of investigation (e.g., Akujor & Garrington 1995; Lüdke et al. 1998). VLBI maps by Simon et al. (1990), Polatidis et al. (1995), and Nan et al. (2000) show a complex structure near the core and a well-resolved jet. There is an abrupt decrease in the jet surface brightness ~10 milliarcsecond (mas) from the core, but the VLBI jet can be followed to a distance of several hundred mas from the core region. The jet remains fairly straight, showing only gentle wiggles before it turns sharply toward the north near the end of its detected length.

Using the 45-m telescope at Nobeyama, Kato et al. (1987) and Inoue et al. (1995) measured a very large integrated rotation measure (RM) for 3C 147 (RM ~ -1500 rad m^{-2}), suggesting that the radio source may be surrounded by a dense medium. VLA polarization observations by Junor et al. (1999) also detected high RM in the main component, RM $= -1300$ rad m^{-2}, indicating the presence of nonuniformity in the gaseous environment of the source. Moreover, 5 GHz VLBA observations obtained in 1995 show that polarization was mostly detected in one bright feature in the inner jet, with the RM of this feature (~ -1300 rad m^{-2}) agreeing with the known high integrated RM of the source (Nan et al. 2000).

However, due to the limited resolution and sensitivity of the previous observations, regions of 3C 147 on parsec scales with significantly different RMs may be averaged together within the 5 GHz beam, leading to depolarization and masking the underlying RM structure. Knowledge of the mas-scale RM distribution is essential to understand the origin of the thermal plasma associated with the high RM and to correctly infer the direction of the underlying magnetic ($\boldsymbol{B}$) field structure, which may be complex. By using four different frequencies in the higher frequency 8 GHz band simultaneously, spatial depolarization will be less and the true distribution of the degree of polarization will be estimated better. The additional resolution provided by the 8 GHz observations may be crucial in recovering the RM distribution on mas scales, which may provide more information about the physical conditions in the VLBI jet, interactions between the jet and its environment, and the properties of the Faraday rotation medium of 3C 147.

A Hubble constant $H_0 = 75$ km s^{-1} Mpc^{-1} and $q_0 = 0.5$ are used throughout this paper. With this choice of the cosmological parameters, at the distance of 3C 147, 1 mas corresponds to 6.5 parsec.

2. Observations and data reduction

Our polarimetric observations of 3C 147 were performed on August 3, 2000 at 8 GHz with the VLBA for about 14 hours. Four sets of two baseband converters (BBCs) (one for RCP and one for LCP in each set) were spaced at four frequencies across the available 8 GHz band which covers 800 MHz. Each BBC corresponded to 8 MHz of bandwidth was recoded with 1-bit sampling. The VLBA correlator produced 16 frequency channels across each BBC bandwidth during every 2-second integration. In this scheme, the simultaneous measurements at the four frequencies (7904, 8238, 8562 and 8888 MHz) have virtually identical u–v coverage, enabling us to obtain simultaneous

Send offprint requests to: H. Y. Zhang,
e-mail: hyzhang@bao.ac.cn

polarization images at these four frequencies in the 8 GHz band. The integrated RM of 3C 147 is ~ -1500 rad m^{-2}, and the variation in the polarization position angle χ caused by such a large RM across an $\simeq$ 980 MHz bandwidth at 8 GHz is $\simeq 25°$.

The data were calibrated, imaged and analyzed using the NRAO AIPS package. During the reduction process, the data at each of the four different frequencies were processed separately. In all steps of the data processing, we used Los Alamos as the reference antenna. The compact source DA193 was selected to determine the feed polarization of the antennas ("D-terms") using the AIPS task LPCAL. The solution shows that the instrumental polarizations are typically of the order of 1%.

The absolute χ calibration was determined using integrated measurements of the polarization angle of the compact polarized source 0300+470 from the Radio Astronomy Observatory Database at the University of Michigan (`http://www.astro.lsa.umich.edu/obs/radiotel/umrao.html`) and observed on September 4, 2000, together with our measurements of the source's total mas-scale polarization. Unfortunately, there are no UMRAO measurements for 0300+470 closer to our observing epoch (August 3, 2000), we therefore had to assume that the polarization of 0300+470 did not vary appreciably in the month between the UMRAO and VLBA observations. We were able to verify our χ calibration by comparing the required polarization PA rotation derived from our calibration with estimates derived for other VLBA polarization observations for which Los Alamos was used as the reference antenna: the right–left phase differences of the individual VLBA antennas are very stable quantities (see, e.g. Reynolds et al. 2003). The polarization-angle rotation derived from our calibration, $\Delta\chi = -55°$, is very close to the values derived for other VLBA polarization observations in October 1997 ($\Delta\chi = -50°$; Reynolds et al. 2003) and March–April 1998 ($\Delta\chi = -46°$; Charlot et al. 2004). Although this does not verify the correctness of our calibration in detail, it does reassure us that our absolute polarization PA calibration is not far off, and should be good to within about 5°. We note also that the integrated rotation measure of 0300+470 is small, and the associated rotation across our 8 GHz band is negligible. Any small inaccuracy in the overall polarization PA calibration therefore will affect only the "de-rotated" χ values, and will not lead to the appearance of spurious rotation measures in the VLBA images.

To obtain the RM distribution, a data cube in λ^2 was first constructed using the AIPS task MCUBE, then the AIPS task RM was used to obtain a weighted fit of the observed χ values to a λ^2 dependence. This procedure also yielded a map of the intrinsic $\boldsymbol{B}$-field vectors, obtained by using the resulting RM distribution to derotate the observed χ values for the VLBI polarization distribution.

3. Results and discussions

3.1. Total intensity and polarization properties

The core region of the total intensity (I) structure of 3C 147 at one of our four frequencies (8238 MHz) is shown in Fig. 1 with a superposition of a grey-scale map of the polarized flux density P in the same region at the same frequency. The I images for the other frequencies are very similar. The very diffuse extended jet to the north roughly 200 mas from the core at 5 GHz was also marginally detected in our 8 GHz observations, and small fraction of flux was picked up at a flux level that is about three times the noise level in the images, which provides not much information about the core.

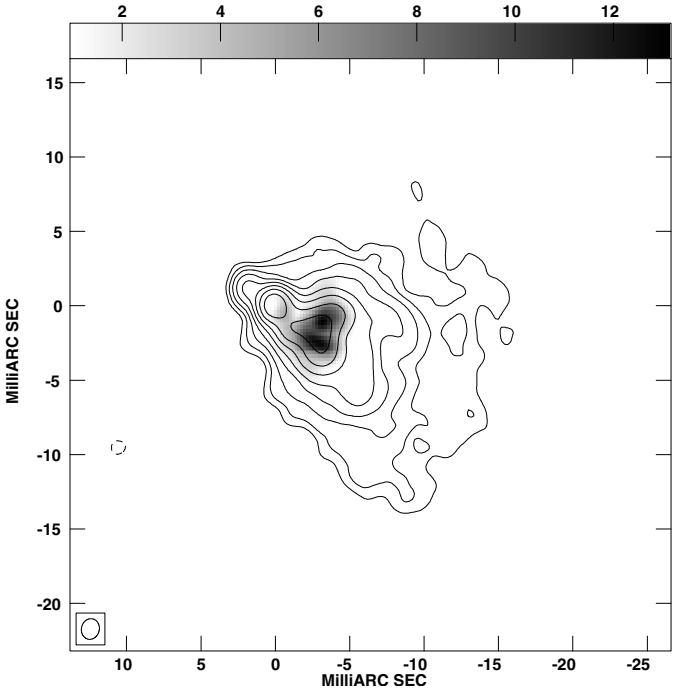

Fig. 1. Gray-scale image of polarized intensity with contours of total intensity at 8238 MHz superimposed. Contour levels are −0.4%, 0.4%, 0.8%, 1.6%, 3.2%, 6.4%, 12.8%, 25.6%, 51.2% of the peak brightness 230 mJy/beam, and the restoring beam shown in the lower left is 1.4 × 1.2 mas at position angle −13°. The gray-scale ranges from 1 to 13.1 mJy/beam.

Gaussian models were fitted to the self-calibrated visibility data using the MODELFIT program in the DIFMAP package. The modelfitting results at the four frequencies are listed in Table 1. The measure of the goodness of fit of the optimized model, the reduced χ^2 at the four frequencies in 8 GHz band, are 1.04, 1.02, 0.91 and 1.06 respectively. The values of the parameters of each component at the four frequencies are quite consistent with each other, and the bandwidth spanned by the frequencies is not large enough to show differences due to the spectral indices of individual components. However, due to the incomplete sampling in the (u, v) plane and the complexity of the source, these models are not unique, and they are not intended to give a detailed description of the VLBI structure. The total flux density in the image in Fig. 1 is about 1.7 Jy, which is about one third of the single-dish flux measured at an earlier epoch by Akujor & Garrington (1995), indicating that a large fraction of the total flux density has been resolved out by the VLBI baselines. We identify the northeast component as the core (component 1), based on its relatively weak polarization (see following text) and its position at one end of the source structure. The peak of the I map corresponds to a bright knot

Table 1. Component parameters in 3C 147.

Frequency (MHz)	Comp.	S (mJy)	Distance (mas)	PA (deg)	Major axis (mas)	Axial ratio	ϕ (deg)	$P_{\rm peak}$ (mJy/beam)	$\chi_{\rm peak}$ (degree)	$m_{\rm peak}$ (percent)
(1)	(2)	(3)	(4)	(5)	(6)	(7)	(8)	(9)	(10)	(11)
7904	1	32	1.92	58	1.37	0.47	46			
	2	224	0.14	60	0.48	0.69	43			
	3	209	1.39	–139	2.28	0.50	17	3.3	–13.9 ± 1.5	3.0
	4	125	2.66	–123	2.19	0.19	–88	7.6	–57.8 ± 0.6	4.7
	5	430	3.72	–127	2.62	0.51	11	10.2	–41.9 ± 0.5	5.9
	6	122	4.07	–97	1.57	0.71	–88	7.8	–75.2 ± 0.6	8.7
	7	478	5.83	–123	7.20	0.76	14			
8238	1	32	1.91	58	1.44	0.41	42			
	2	222	0.14	59	0.48	0.69	39			
	3	206	1.36	–140	2.29	0.49	18	4.3	–4.8 ± 0.9	3.8
	4	129	2.66	–124	2.21	0.20	–87	8.9	–48.3 ± 0.5	5.5
	5	428	3.73	–127	2.63	0.51	11	11.7	–35.0 ± 0.4	6.8
	6	117	4.06	–98	1.57	0.69	–89	9.0	–67.6 ± 0.4	10.0
	7	507	5.74	–123	7.51	0.74	15			
8562	1	28	1.94	58	1.33	0.35	44			
	2	222	0.15	58	0.47	0.69	41			
	3	208	1.35	–140	2.29	0.49	18	4.6	5.8 ± 1.1	4.1
	4	131	2.67	–123	2.23	0.21	–87	9.2	–38.0 ± 0.6	5.6
	5	428	3.72	–127	2.64	0.50	11	11.8	–23.1 ± 0.4	6.9
	6	118	4.06	–97	1.57	0.71	87	9.0	–58.3 ± 0.6	10.1
	7	497	5.82	–123	7.40	0.75	14			
8888	1	26	1.93	57	1.28	0.28	48			
	2	220	0.15	58	0.42	0.75	40			
	3	222	1.35	–141	2.34	0.50	18	4.9	10.5 ± 1.0	4.4
	4	131	2.68	–123	1.96	0.27	–87	10.5	–28.1 ± 0.5	6.4
	5	418	3.76	–127	2.61	0.50	11	13.5	–15.6 ± 0.4	7.8
	6	125	4.08	–98	1.62	0.72	86	10.5	–50.1 ± 0.5	11.9
	7	480	5.87	–123	7.26	0.76	13			

Notes: The columns present the (1) Observing frequency; (2) Component; (3) Total flux density of each component; (4), (5) Offset (distance and position angle) of each component from the image phase center; (6), (7) and (8) Major axis (FWHM), axial ratio and position angle of major axis of each elliptical component; (9), (10) and (11) Polarized flux density, polarization position angle with 3σ error and ratio of P to I flux (m) at the peak location of each component.

in the jet. The bulges toward the northwest and southwest visible in the 5 GHz VLBA images of Nan et al. (2000) are more prominent in our 8 GHz map, and exhibit a distorted morphology, suggesting they are associated with the interaction of the inner jet with the ambient gas. Similar structures have also been detected by Fey & Charlot (2000) in VLBA images obtained at 8550 MHz, supporting the reality of these extended emission features.

Polarization of 3C 147 was detected mainly in the distorted region of the inner jet. In Fig. 1, the knotty polarization structure at 5 GHz observation by Nan et al. (2000) has been resolved into two main polarized components which are coincident with the bulges of the inner jet toward the northwest and southwest.

Table 1 gives the polarized flux densities (P), polarization position angles (χ), and ratios of P to I flux (m) at the central positions of four Gaussian components, where $P = (Q^2 + U^2)^{1/2}$, $\chi = 1/2 \arctan(U/Q)$ and I, Q, U are the corresponding Stokes parameters. We have not carried out these calculations for the other three components, whose P peak flux densities are smaller than 1 mJy/beam in the P image. The degrees of polarization m for each component in Table 1 show a tendency to increase with increasing frequency. If this increase in m across our bandwidth is real, this may represent depolarization due to the thermal plasma that is giving rise to the large RM in this region.

Since the peak of the polarized emission is offset from the I peak, the m values given in Table 1 are only approximations to the percentage polarization associated with a particular component. The total polarization on VLBI scales derived from the total fluxes in the Q and U maps is about 42 mJy, which is also nearly one-third of the integrated 8 GHz polarized flux intensity observed with VLA by Akujor & Garrington (1995) at an earlier epoch (150 mJy), indicating that most of the polarized flux has been resolved by the VLBI baselines. The overall degree of polarization for the polarized region of 3C 147 is about 6%,

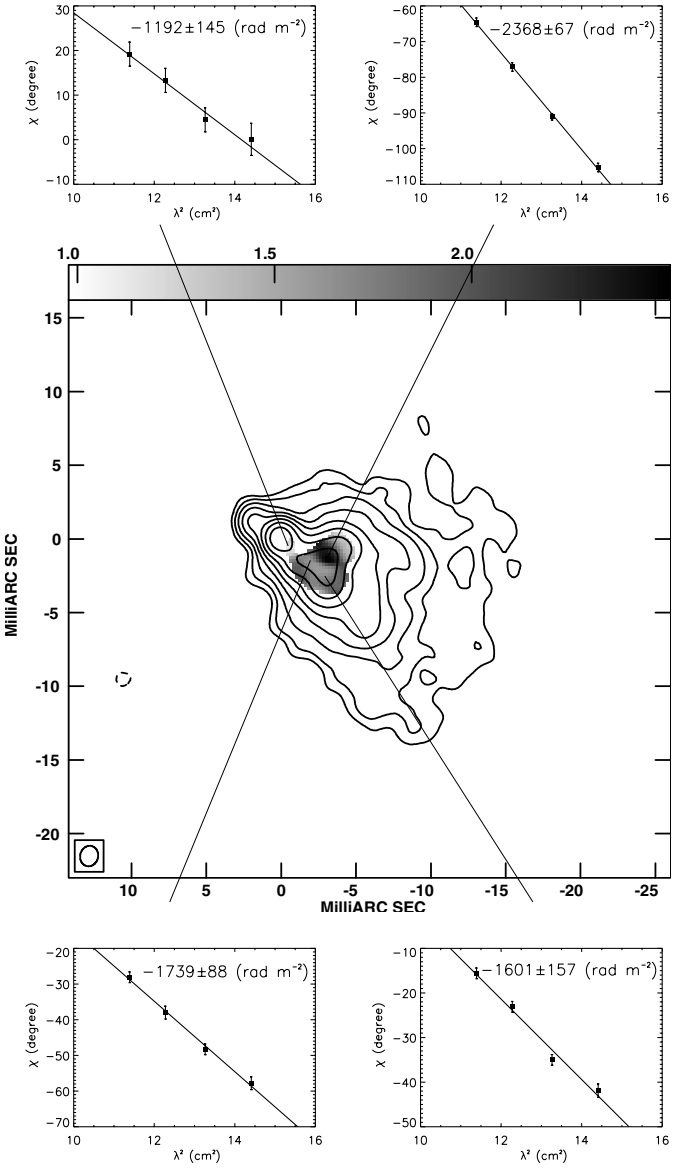

Fig. 2. Gray-scale image of Rotation Measure with contours of total intensity at 8238 MHz superimposed. Contours are as in Fig. 1. The uncertainty in the local rotation measure is less than ±100 rad m^{-2}. The gray-scale ranges from 985 to 2496 rad m^{-2}, the actual value of the RM is the negative of that in the gray-scale map. The four inserts show plots of χ vs. λ^2 (units of cm^2).

three times higher than that observed in the 5 GHz VLBA observations (Nan et al. 2000).

3.2. Rotation measure and intrinsic magnetic fields

Figure 2 presents the mas-scale RM distribution of 3C 147, together with plots of the RM fit over 8 GHz band at four different points within the polarized region. The uncertainty of the χ values in Fig. 2 was calculated from the rms noise of the Q and U maps at the four frequencies, and the error bars shown in Fig. 2 are 3σ. No redshift corrections have been applied to the wavelengths, so the RMs in the rest frame of 3C 147 are higher by a factor of $(1 + z)^2$. The RM values in Fig. 2 range from −985 to −2496 rad m^{-2}. If the variation of χ at our four

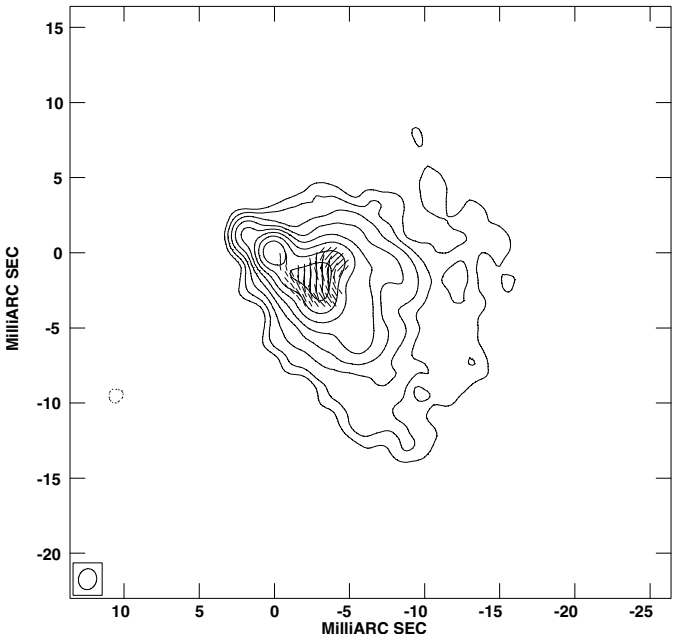

Fig. 3. Contour image of total intensity at 8238 MHz with ***B***-field vectors (corrected for the RMs shown in Fig. 2) overlaid. Contours are as in Fig. 1.

frequencies is associated with Faraday rotation, the χ values should form a straight line when plotted as a function of λ^2. A linear least-squares fit for χ vs. λ^2 was obtained for each of the four locations in the source. The results show that the χ variations for these four points are described well by a λ^2 dependence, implying the presence of Faraday rotation.

Recent VLBI polarimetry observations for the CSS quasars 3C 119 (Nan et al. 1999), 0548+165 and 1524-136 (Mantovani et al. 2002) have detected high RMs on mas scales in these sources as well, implying that the high RMs are not due to foreground plasma in the Milky Way, and are probably associated with the collision of the VLBI jet with a dense thermal plasma in the immediate vicinity of the source. We can see that the mas-scale RM distribution of 3C 147 is likewise not uniform, demonstrating that the thermal gas giving rise to the observed Faraday rotation is located in the immediate vicinity of the jet. The highest RMs are observed in the north polarized region, and are associated with the northern bulge of the distorted jet in the total intensity map. Combining the distorted structure of the inner jet, the observed depolarization and the good λ^2 RM fits, we suggest that the large RM may be produced by a cocoon surrounding the radio jet. This cocoon may be densest around the northern bulge in the inner jet, preventing the further expansion of the inner jet to the northwest, leading to the distortion of the jet in the core region.

The RM-corrected magnetic-field orientation distribution is shown in Fig. 3. To obtain this ***B***-field map, the observed χ values have been "de-rotated" to their intrinsic values using the derived RM distribution, then rotated by 90°, assuming that the observed polarized regions are optically thin. This is a good assumption in this case, since the polarized region is in the jet, well separated from the core, and displays fairly high degrees of polarization.

The magnetic-field structure is complex; it is roughly consistent with the ***B***-field map found at 5 GHz by Nan et al. (2000), but shows appreciably more structure due to the increased resolution of our 8 GHz observations. Over much of the jet in the vicinity of components 4, 5 and 7, the ***B***-field runs roughly along the jet direction, as is most typical of the VLBI jets of quasars. At the same time, the ***B***-field in the central spine of the jet is oblique to the jet direction, possibly suggesting the presence of a shocked region. It is difficult to interpret the ***B***-field orientation in the northern polarized region relative to the local flow of jet material there. Taking into account the *I* morphology and the fact that the highest RM is in this northern formation, it may be that the VLBI jet of 3C 147 is sharply deflected toward the north by a dense surrounding medium in this region. In this case, it is possible that the ***B***-field vectors in the northwest bulge are aligned with the local jet flow direction (toward the northwest).

4. Conclusions

Using VLBA polarimetry of 3C 147 at several frequencies within the 8 GHz band, we have derived the total intensity, polarization and rotation-measure distributions of the source on parsec scales. The source polarization is clearly resolved into three main polarized regions corresponding to the central region of the jet and a bulge of the distorted inner jet toward the northwest.

The RM values derived from the four-frequency data on a pixel-by-pixel basis range from about -985 to -2500 rad m^{-2}, showing that the RM distribution is non-uniform on mas scales, so that the thermal plasma causing the Faraday rotation is located in the immediate vicinity of the VLBI jet. The highest RM value is measured near the peak of the northern polarized component. We suggest that the material causing the high RMs in 3C 147 is associated with a cocoon of thermal plasma surrounding the jet, which appears to be densest in the northern region of the inner jet.

The ***B***-field derived by correcting the observed polarization vectors for the derived RM distribution is aligned with the jet extending to the southwest along part of the jet, but also shows a region of oblique ***B***-field in part of the spine of the inner jet, possibly indicating the action of a shock. The ***B***-field in the northern polarized region is oriented toward the northwest, and may reflect the direction of the local jet if part of the inner jet has been sharply deflected by the interaction of the jet with the dense surrounding medium.

Acknowledgements. Haiyan Zhang would like to thank the Joint Institute for VLBI in Europe (JIVE) for its hospitality and financial assistance during her visit, and also thank Dr. Leonid Gurvits, Dr. Michael Garrett, Dr. Cormac Reynolds, Dr. Ian M. Avruch, Dr. Bob Campbell and Dr. Hiroshi Imai for their useful discussions and kind help. This work is supported partly by the grants from the National Natural Science Foundation (NSFC10173015, NSFC10303003) and the NKBRSF(2003CB716703) in China. The authors acknowledge support from the exchange program of the Chinese and Dutch Academies of Sciences. The National Astronomy Observatory (NRAO) is a facility of the National Science Foundation operated under cooperative agreement by Associated Universities, Inc. This research has used the data from the University of Michigan Radio Astronomy Observatory which is supported by funds from the University of Michigan.

References

Akujor, C. E., & Garrington, S. T. 1995, A&AS, 112, 235
Charlot, P., Gabuzda, D. C., Sol, H., Degrange, B., & Piron, F. 2004, to be submitted to A&A
Fey, A. L., & Charlot, P. 2000, ApJS, 128, 17
Inoue, M., Tabara, H., Kato, T., & Aizu, K. 1995, PASJ, 47, 725
Junor, W., Salter, C. J., Saikia, D. J., Mantovani, F., & Peck, A. B. 1999, MNRAS, 308, 955
Kato, T., Tabara, H., Inoue, M., & Aizu, K. 1987, Nature, 329, 223
Lüdke, E., Garrington, S. T., Spencer, R. E., et al. 1998, MNRAS, 299, 467
Mantovani, F., Junor, W., Ricci, R., et al. 2002, A&A, 389, 58
Nan, R. D., Gabuzda, D. C., Kameno, S., Schilizzi, R. T., & Inoue, M. 1999, A&A, 344, 402
Nan, R. D., Zhang, H. Y., Gabuzda, D. C., et al. 2000, A&A, 357, 891
Polatidis, A. G., Wilkinson, P. N., Xu, W., et al. 1995, ApJS, 98, 1
Reynolds, C., Cawthorne, T. V., & Gabuzda, D. C. 2001, MNRAS, 327, 1071
Simon, R. S., Readhead, A. C. S., Moffet, A. T., et al. 1990, ApJ, 354, 140